SEARCH FOR SUPERSYMMETRIC PARTNERS OF ELECTRONS

JADE Collaboration

W. BARTEL, L. BECKER, C. BOWDERY [1], D. CORDS [2], R. FELST, D. HAIDT, H. JUNGE [3], G. KNIES, H. KREHBIEL, P. LAURIKAINEN [4], R. MEINKE, B. NAROSKA, J. OLSSON, D. SCHMIDT [3], P. STEFFEN

Deutsches Elektronen-Synchrotron DESY, Hamburg, Germany

G. DIETRICH, J. HAGEMANN, G. HEINZELMANN, H. KADO, C. KLEINWORT, M. KUHLEN, K. MEIER, A. PETERSEN [2], R. RAMCKE, U. SCHNEEKLOTH, G. WEBER

II. Institut für Experimentalphysik der Universität Hamburg, Hamburg, Germany

K. AMBRUS, S. BETHKE, A. DIECKMANN, J. HEINTZE, K.H. HELLENBRAND, R.D. HEUER [5], S. KOMAMIYA, J. VON KROGH, P. LENNERT, H. MATSUMURA, H. RIESEBERG, J. SPITZER, A. WAGNER

Physikalisches Institut der Universität Heidelberg, Heidelberg, Germany

A. FINCH, F. FOSTER, G. HUGHES, T. NOZAKI [6], J. NYE

University of Lancaster, Lancaster, England

J. ALLISON, J. BAINES, A.H. BALL, R.J. BARLOW, J. CHRIN, I.P. DUERDOTH, T. GREENSHAW, P. HILL, F.K. LOEBINGER, A.A. MACBETH, H. McCANN, H.E. MILLS, P.G. MURPHY, K. STEPHENS, P. WARMING

University of Manchester, Manchester, England

R.G. GLASSER, B. SECHI-ZORN, J.A.J. SKARD, S.R. WAGNER, G.T. ZORN

University of Maryland, MD, USA

S.L. CARTWRIGHT, D. CLARKE, R. MARSHALL, R.P. MIDDLETON, J.B. WHITTAKER

Rutherford Appleton Laboratory, Chilton, England

T. KAWAMOTO, T. KOBAYASHI, T. MASHIMO, M. MINOWA, H. TAKEDA, T. TAKESHITA and S. YAMADA

International Center for Elementary Particle Physics, University of Tokyo, Tokyo, Japan

Received 10 December 1984

[1] European Science Exchange Fellow.
[2] Present address: SLAC, CA, USA.
[3] Universität-Gesamthochschule Wuppertal, Wuppertal, Germany.
[4] University Helsinki, Helsinki, Finland.
[5] Present address: CERN, Geneva, Switzerland.
[6] Present address: KEK, Ibaraki, Japan.

A search for the supersymmetric partners of the electron was made assuming different photino masses. If both types of scalar electrons have an equal mass and the photino is massless, then the lower limit of the scalar electron mass was found to be 25.2 GeV/c^2, whereas, if the scalar electrons have different masses, the lower limit is 21.8 GeV/c^2.

Supersymmetric theories [1] have been attracting considerable attention recently, especially in connection with understanding the gauge hierarchy problem [2] and its applications to grand unified theories and cosmology [3]. Supersymmetric theories assume the existence of a set of particles corresponding to all known particles which have spins differing by one-half from those of the partner particles. For instance, there could be scalar leptons, $\tilde{\ell}_L$ and $\tilde{\ell}_R$, which are the partners of left-handed and right-handed leptons ℓ, respectively, and a spin 1/2 photino, $\tilde{\gamma}$, which is the partner of the photon. Since the couplings between the supersymmetric particles and the ordinary particles are well-defined in supersymmetric theories, although some of them are model-dependent, the production cross sections and the decay rates of the supersymmetric particles can be calculated. The masses of the supersymmetric particles, however, cannot be predicted by the supersymmetric theories. Some theories [4] predict $M(\tilde{\ell}_L) = M(\tilde{\ell}_R)$ and an almost massless photino, while others [5] predict $M(\tilde{\ell}_L) > M(\tilde{\ell}_R)$ and a heavy photino.

Experimental searches for supersymmetric scalar electrons have been performed in electron and positron collisions by the PETRA and PEP experiments [6,7] and lower limits of the mass have been obtained. PETRA experiments used the pair production process assuming a massless photino. They obtained lower limits of the mass ranging between 13 and 16.8 GeV/c^2. Recently PEP experiments made a scalar electron search through the single scalar electron production process ($e^+e^- \to e\tilde{e}\tilde{\gamma}$) [8]. The MARK-II and MAC collaborations obtained lower mass limits of 22.2 and 22.4 GeV/c^2, respectively, assuming $M(\tilde{e}_L) = M(\tilde{e}_R)$ and $M(\tilde{\gamma}) = 0$.

In this paper we describe a model-independent search for scalar electrons which has been made by using the JADE detector at PETRA. We studied all possible cases for the masses of the scalar electrons and the photino. We assume that the photino is stable and not interacting so that it is invisible. If the photino is massive, it may decay into γ + G (goldstino) with a lifetime which is model-dependent [9]. In such a case a better limit on the masses of $\tilde{e}$ and $\tilde{\gamma}$ can be obtained by the process $e^+e^- \to \tilde{\gamma}\tilde{\gamma}$ [10–12] rather than the processes described here. A preliminary result of this work has been reported before [13] and a similar search for scalar muons has been performed [14]. In the following, we first describe a search for one type of scalar electron (e.g. $\tilde{e}_R$), and then the equal mass case for both types of scalar electron.

A detailed description of the experimental apparatus has been given in previous publications [15]. The important parts of the detector for this analysis are the inner cylindrical drift chamber ("jet chamber") which measures momenta and dE/dx of charged particles and has up to 48 sampling points along a track, time of flight counters (TOF) with a time resolution of ~0.4 nsec, an array of lead glass shower counters covering 90% of the full solid angle and 5 layers of drift chambers and absorbers for muon identification. The relevant trigger for the following analyses is the total shower energy trigger which is the sum of the energies deposited in the lead glass counters having the threshold of ~3–4 GeV. We used data collected up to spring 1984 with center of mass energies ($\sqrt{s}$) between 32.0 and 46.78 GeV, and an integrated luminosity $\int \mathcal{L}\,dt = 87.2\ \text{pb}^{-1}$.

$\tilde{e}_R$ search

Three types of analysis (A, B, C) for the $\tilde{e}_R$ search are described. Types A and B use pair production, and type C uses an indirect method. The same results apply to $\tilde{e}_L$. The cross section for $e^+e^- \to \tilde{e}_R\bar{\tilde{e}}_R$ with a finite photino mass is used as given by [16]

$$d\sigma/d\cos\vartheta = (\pi\alpha^2/8s)\,\beta^3 \sin^2\vartheta \times \{1 + [1 - 4/(1 - 2\beta\cos\vartheta + \beta^2 + \mu^2)]^2\}, \quad (1)$$

where $\mu = M(\tilde{\gamma})/E_{\text{beam}}$, $\beta^2 = 1 - [M(\tilde{e})/E_{\text{beam}}]^2$ and E_{beam} is the beam energy.

Analysis A: $\tilde{e}_R\bar{\tilde{e}}_R$-pair production with $M(\tilde{e}_R) > M(\tilde{\gamma})$. As the scalar electron decays into $e + \tilde{\gamma}$ in this case, with a lifetime which is expected to be very short (typically ~10^{-23} s) [17], the signature of the event is an acoplanar e^+e^- pair and no other particles. The selection criteria were as follows:

(1) two clusters in the lead glass counters, each with $E > E_{beam}/4$ and $|\cos\vartheta| < 0.75$, where E and ϑ are the energy and polar angle of a cluster;

(2) the other clusters must have energies less than 1 GeV;

(3) the acollinearity angle, i.e. the supplementary angle between the directions of the two big clusters, $> 10°$;

(4) acoplanarity angle, i.e. the supplementary angle between the projected directions of the two big clusters in the plane perpendicular to the beam axis, $> 10°$;

(5) $2 \leqq$ number of charged tracks in the jet chamber $\leqq 10$;

(6) $R_{min}(\text{event}) < 10$ mm and $|Z_{min}(\text{event})| < 100$ mm. For each track the closest point from the origin (i.e. the center of the detector) was determined. The R- and z-coordinates of the point are called R_{min} and Z_{min}, respectively. $R_{min}(\text{event})$ and $|Z_{min}(\text{event})|$ are the minimum values of R_{min} and $|Z_{min}|$ for all tracks in an event;

(7) no good tracks outside 10° cones around the two big clusters, where a good track means: the number of hits in the jet chamber $\geqq 24$, $R_{min} < 10$ mm, $|Z_{min}| < 100$ mm, and momentum $p > 200$ MeV/c;

(8) there must be at least one track inside each of the 10° cones around the two big clusters. This condition ensures that the two big clusters are not photons;

(9) $|(\text{missing mass})^2| > 70\ (\text{GeV})^2$ or $|\cos\vartheta\ (\text{missing momentum})| < 0.7$, where the missing mass and the missing momentum are calculated from the two big clusters. This cut is applied in order to reject eeγ events where the γ cannot be detected.

After these cuts 85 events survived. They were visually scanned to select only the clean events with an electron and a positron and nothing else. The innermost layer of the muon chambers and the forward muon counters were looked at to see if there were any photons which passed through the gaps between lead glass blocks and initiated electromagnetic showers in the magnet iron. Two photon events were rejected if they showed hits in the forward shower counters.

After the scan 13 events were left, which could be considered as $e^+e^- \to e^+e^-\gamma\gamma$ events where both photons escaped the detector. The acoplanarity angle distribution of these events is shown in fig. 1 (hatched histogram). Fig. 1 also shows the distributions expected for $e^+e^- \to \tilde{e}_R\bar{\tilde{e}}_R \to e^+e^- + \ldots$ calculated by

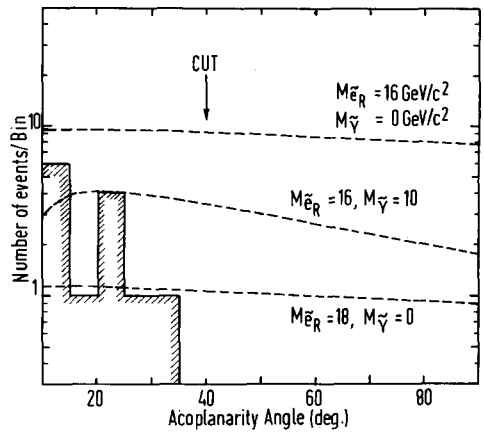

Fig. 1. Observed acoplanarity angle distribution for $e^+e^- \to e^+e^-$ + missing energy. Dashed lines are the expected distributions for $e^+e^- \to \tilde{e}_R\bar{\tilde{e}}_R \to e^+e^- + \ldots$, where $M(\tilde{e}_R) = 16$ and 18 GeV/c^2 with $M(\tilde{\gamma}) = 0$ GeV/c^2, and $M(\tilde{e}_R) = 16$ GeV/c^2 with $M(\tilde{\gamma}) = 10$ GeV/c^2. The final cut on the acoplanarity angle is also indicated by an arrow (= 40°).

Monte Carlo simulation for various assumptions on $M(\tilde{e}_R)$ and $M(\tilde{\gamma})$ applying the same cuts as above. No events were observed at an acoplanarity angle above 40°. This observation allows us to exclude with 95% confidence level the shaded area in the $(M(\tilde{e}_R), M(\tilde{\gamma}))$ plane under the curve (A) in fig. 2a.

Analysis B: $\tilde{e}_R\bar{\tilde{e}}_R$-pair production with $M(\tilde{e}_R) < M(\tilde{\gamma})$. If $\tilde{e}_R$ is the lightest of all the supersymmetric particles, it would be stable and the event would look like heavy muon pair production. If the scalar electron mass is small but heavier than several MeV/c^2, this process is hardly distinguishable from $e^+e^- \to \mu^+\mu^-$, and it could be observed as an increase of $\sigma(e^+e^- \to \mu^+\mu^-)$. JADE has already presented results on $\sigma(e^+e^- \to \mu^+\mu^-)$ [18], which showed that the measured cross section at $\langle\sqrt{s}\rangle = 34.46$ GeV is consistent with the QED prediction with a statistical error of 1.8% and a systematic error of 5%. From that we could exclude the region, $M(\tilde{e}_R) < 9.4$ GeV/c^2, for the stable $\tilde{e}_R$ with 95% confidence level.

If the scalar electron mass is high, it can be identified by measuring its velocity by TOF counters and/or by dE/dx measurement. Starting from the data set of muon pair candidates [18] with relaxed TOF cuts ($\sqrt{s} \approx 34.5$–39.2 GeV, $\int \mathcal{L}dt = 39.9$ pb^{-1}), for which

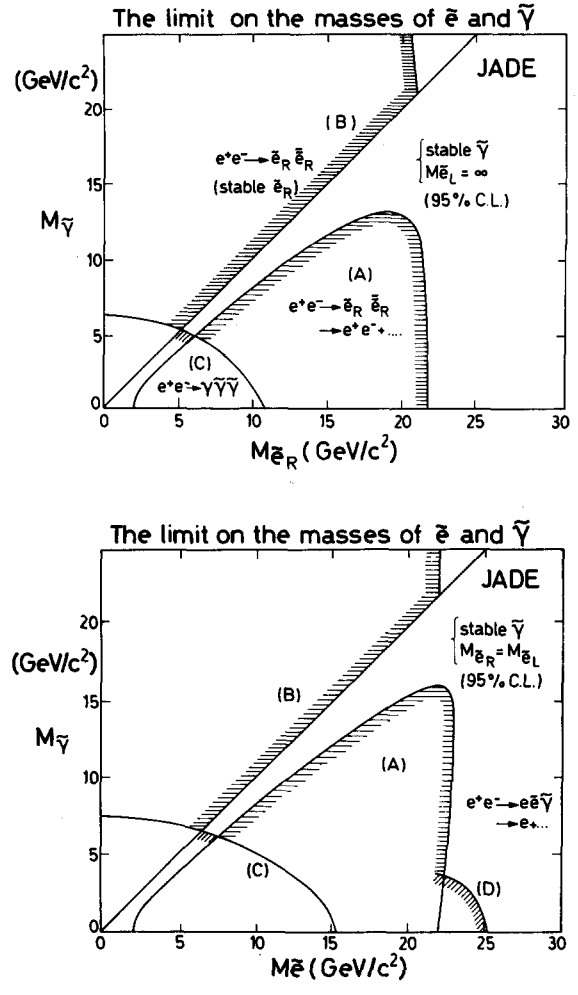

Fig. 2 (a) Excluded regions for $M(\tilde{e}_R)$ and $M(\tilde{\gamma})$ by the analyses A, B and C (see text) in case of $M(\tilde{e}_L) = \infty$. (b) Excluded regions for $M(\tilde{e})$ and $M(\tilde{\gamma})$ by the analyses A, B, C and D in case of $M(\tilde{e}_R) = M(\tilde{e}_L)$.

the selection criteria were essentially coplanar non-showering particle pair with $p > E_{beam}/3$ and $|\cos\vartheta| < 0.76$ for both tracks, the following additional cuts were applied:

$$1/3 < \beta_1, \beta_2 < 0.85, \quad |\beta_1 - \beta_2| < 0.4\,\beta_{av}^2,$$

where β_1 and β_2 are the velocities (normalized to the velocity of light) and $\beta_{av} = (\beta_1 + \beta_2)/2$. There remained 16 events, which could be explained as a tail of muon pair production events or cosmic ray events. However, they were taken as real events in obtaining a mass limit. From a Monte Carlo simulation including the above cuts the excluded region is obtained to be $7.7\ \text{GeV}/c^2 < M(\tilde{e}_R) < 15.7\ \text{GeV}/c^2$ for the stable $\tilde{e}_R$.

The dE/dx information provides a clear signal for a heavy charged particle with $\beta < 0.7$. To a similar muon data set which includes data at the highest PETRA energy ($\sqrt{s} \approx 34.5$–46.78 GeV, $\int \mathcal{L}\,dt = 64.8\ \text{pb}^{-1}$) the following tighter cuts were applied:

$$\beta_1, \beta_2 < 0.7, \quad |\beta_1 - \beta_2| < 0.4\,\beta_{av}^2,$$

$dE/dx > 10$ keV/cm for both tracks.

No events were observed. The dE/dx cut is equivalent to $\beta < 0.7$ for $\tilde{e}_R\tilde{e}_R$-pair production. Excluded mass region in the $(M(\tilde{\gamma}), M(\tilde{e}_R))$ plane was obtained by Monte Carlo simulations. Although the higher limit of the excluded region depends slightly on $M(\tilde{\gamma})$ [see the boundary (B) in fig. 2a], the region $12.4\ \text{GeV}/c^2 < M(\tilde{e}_R) < 20.3\ \text{GeV}/c^2$ was excluded for the stable $\tilde{e}_R$ for any value of $M(\tilde{\gamma})$.

Combining the above three results, the shaded area (b) in fig. 2a is excluded at 95% confidence level. The minimum lower limit on the mass of $M(\tilde{e}_R)$ is 20.3 GeV/c^2 for $M(\tilde{\gamma})$ $(> M(\tilde{e}_R))$.

Analysis C: $e^+e^- \to \gamma\tilde{\gamma}\tilde{\gamma}$. This process can also be used to obtain a limit on the masses of a scalar electron and a photino. This process occurs through the diagrams shown in fig. 3, and the cross section was calculated in ref. [19] for finite photino masses. Since the photino is assumed to be stable, the signature of the event is a single photon with nothing else.

The single photon event search has already been made in our previous publication [11] in conjunction with the (unstable) photino search through the process, $e^+e^- \to \tilde{\gamma}\tilde{\gamma}$ where one of the photinos decays into $\gamma + G$. There were no events observed after the selection cuts

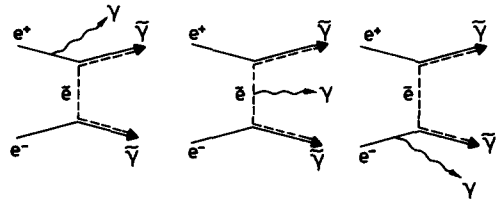

Fig. 3. Feynman diagrams relevant to the process $e^+e^- \to \gamma\tilde{\gamma}\tilde{\gamma}$.

(the main cut was $p_T > 0.6\, E_{beam}$) [11].

This analysis can be applied to the process $e^+e^- \to \gamma\tilde{\gamma}\tilde{\gamma}$ in the case of a stable photino. A Monte Carlo simulation was made using the cross section formula in ref. [19]. The result is shown in fig. 2a [region (C)] indicating that a part of the narrow gap between the regions excluded by analyses A and B is rejected.

Combining the above three analyses A, B and C, a scalar electron with a mass below 5.3 GeV/c^2 is excluded, independent of the photino mass. If the photino is massless, the lower limit of $M(\tilde{e}_R)$ is 21.8 GeV/c^2.

Equal mass case

If the beam energy of the e^+e^- colliding machine exceeds the masses of both types of scalar electrons, both of them will be pair-produced, where not only $\tilde{e}_R\bar{\tilde{e}}_R$ and $\tilde{e}_L\bar{\tilde{e}}_L$ but also $\tilde{e}_R\bar{\tilde{e}}_L$ and $\tilde{e}_L\bar{\tilde{e}}_R$ can be produced. The cross section for $e^+e^- \to \tilde{e}\bar{\tilde{e}}$ ($= \tilde{e}_R\bar{\tilde{e}}_R + \tilde{e}_L\bar{\tilde{e}}_L + \tilde{e}_R\bar{\tilde{e}}_L + \tilde{e}_L\bar{\tilde{e}}_R$) in case of $M(\tilde{e}_R) = M(\tilde{e}_L)$ and a finite photino mass was calculated to be [16,20]

$$d\sigma/d\cos\vartheta = (\pi\alpha^2/4s)[\beta^3 \sin^2\vartheta \times \{1 + [1 - 4/(1 - 2\beta\cos\vartheta + \beta^2 + \mu^2)]^2\} + 16\mu^2\beta/(1 - 2\beta\cos\vartheta + \beta^2 + \mu^2)^2]. \quad (2)$$

For the more general case (i.e. arbitrary masses for $\tilde{e}_R$, $\tilde{e}_L$ and $\tilde{\gamma}$) the cross section formula is given in ref. [16]. The second term in the square bracket in formula (2) comes from the process $e^+e^- \to \tilde{e}_R\bar{\tilde{e}}_L + \tilde{e}_L\bar{\tilde{e}}_R$, which vanishes for the massless photino. Hence, we gain sensitivity if the photino is massive, as $\sigma(e^+e^- \to \tilde{e}\bar{\tilde{e}}) > \sigma(e^+e^- \to \tilde{e}_R\bar{\tilde{e}}_R + \tilde{e}_L\bar{\tilde{e}}_L)$. For the process $e^+e^- \to \gamma\tilde{\gamma}\tilde{\gamma}$, its cross section for the case $M(\tilde{e}_L) = M(\tilde{e}_R)$ is just twice as much as that for the case of $M(\tilde{e}_L) = \infty$ [19].

By using the cross section formula for the equal mass case for $\tilde{e}_R$ and $\tilde{e}_L$, we repeated the above analyses A, B and C. The results are shown in fig. 2b. The excluded region (D) was obtained by the analysis described below. (This analysis was also made in the case of $\tilde{e}_R$ search, but the excluded region did not exceed the region obtained by other analyses.)

Analysis D: $e^+e^- \to e\tilde{e}\tilde{\gamma} \to e +$ .... The process $e^+e^- \to e\tilde{e}\tilde{\gamma}$ offers an opportunity to search for a scalar electron with a mass higher than the beam energy. Here the scalar electron is singly produced by the scattering of an initially radiated photon and an electron. The $e^\pm$ which radiates the photon goes mostly along the beam direction, and it is not observed. So the final state to be observed is a single electron coming from the $\tilde{e}$-decay with no other particles. The cross section for this process was originally calculated in ref. [8] using the Weizsäcker–Williams approximation and assuming a massless photino. It was generalized for a massive photino in ref. [16].

We analysed data at CM energies of $\sqrt{s} \approx 32$–38.6 GeV and $\int \mathcal{L}\,dt = 72.8$ pb^{-1} to find any single electron events. The selection criteria were as follows:

(1) one cluster with $E > E_{beam}/4$, $|\cos\vartheta| < 0.7$ and $|\varphi - 90°(270°)| > 25°$;

(2) residual energy < 1 GeV;

(3) $1 \leqq$ number of charged tracks $\leqq 10$;

(4) number of good tracks $\geqq 1$ (good track: number of hits $\geqq 24$, $R_{min} < 20$ mm, $|Z_{min}| < 200$ mm and $p > 100$ MeV/c);

(5) R_{min}(event) < 10 mm and $|Z_{min}$(event)$| < 100$ mm;

(6) number of hits in the jet chamber $\leqq 400$;

(7) no good tracks outside a 10° cone around the biggest cluster;

(8) at least one track in the 10° cone around the biggest cluster;

(9) no hits in the innermost layer of the muon chambers opposite to the electron within the azimuthal angle range of ±10°.

The azimuthal angle (φ)-cut was applied to avoid the hole in the innermost layer of the muon chambers, which had to be used in cut (9) to reject $e^+e^- \to \gamma\gamma$ events where one photon converts in the beam pipe and the other photon goes through a gap between the lead glass counters. The events which passed these cuts were mostly from the process $e^+e^- \to e^+e^-\gamma$, where one of the electrons and the photon escaped the detector. We scanned the events with $p_T > 0.55\, E_{beam}$, where p_T = (cluster energy) × $\sin\vartheta$. Several events were rejected by the scan, as they had signs of particles besides the electron in the forward counters, the innermost end wall muon chambers or the jet chamber. Fig. 4 shows the p_T distribution of the remaining events (hatched histogram). No events are seen for $p_T > 0.65\, E_{beam}$. The expected p_T distribution for $e^+e^- \to e\tilde{e}\tilde{\gamma} \to e +$ ... with $M(\tilde{e}) = 22$ GeV/c^2 and $M(\tilde{\gamma}) = 0$ GeV/c^2 (to be multiplied by 1/200) is indicated also

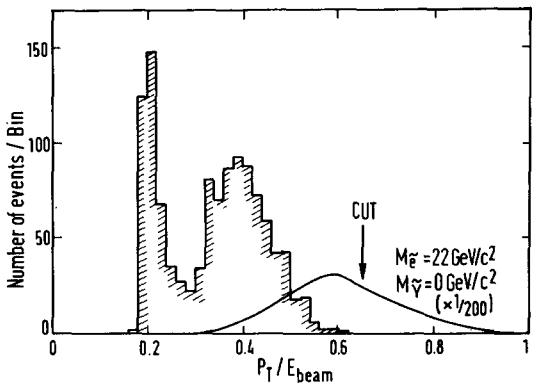

Fig. 4. Observed p_T distribution of an electron for $e^+e^- \to e^\pm$ + missing energy. The curve shows the expected distributions for $e^+e^- \to e\tilde{e}\tilde{\gamma} \to e$ + ..., with $M(\tilde{e}) = 22$ GeV/c^2 and $M(\tilde{\gamma}) = 0$ GeV/c^2. The cut was chosen to be $p_T/E_{beam} = 0.65$.

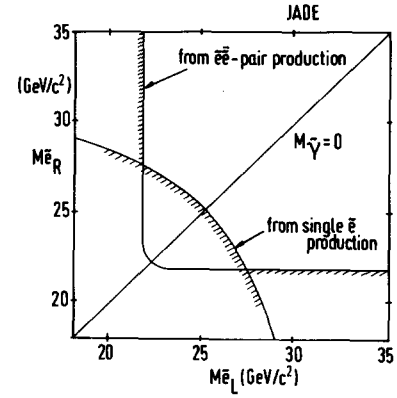

Fig. 5. Excluded regions for $M(\tilde{e}_R)$ and $M(\tilde{e}_L)$ in case of $M(\tilde{\gamma}) = 0$ GeV/c^2.

in fig. 4. Thus, we could exclude the region (D) in fig. 2b.

Combining the analyses A, B, C and D for the equal mass case, $M(\tilde{e}) > 6.5$ GeV/c^2, independent of the photino mass. If the photino is massless, the lower limit of $M(\tilde{e})$ is 25.2 GeV/c^2.

Finally we quote the excluded mass region in the $(M(\tilde{e}_L), M(\tilde{e}_R))$ plane for the case of a massless photino. The mass limits for $\tilde{e}_R$ and $\tilde{e}_L$ were obtained from the analyses of the $\tilde{e}\tilde{e}$-pair production and the single $\tilde{e}$ production. The hatched area in fig. 5 is excluded.

Conclusions

We have searched for the supersymmetric partners of the electron assuming a stable photino with arbitrary mass. We analysed the processes $e^+e^- \to \tilde{e}\tilde{e}$, $e^+e^- \to \gamma\tilde{\gamma}\tilde{\gamma}$ and $e^+e^- \to e\tilde{e}\tilde{\gamma}$, and found no signs of such particles. Limits on the masses of $\tilde{e}_R$, $\tilde{e}_L$ and $\tilde{\gamma}$ were obtained. If only one type of scalar electron is considered, e.g. $M(\tilde{e}_L) = \infty$, the lower limit of $M(\tilde{e}_R)$ is 21.8 GeV/c^2 (95% confidence level) for the massless photino. In case that both types of scalar electron have the same mass, the limit is $M(\tilde{e}) > 25.2$ GeV/c^2 for the massless photino.

We are indebted to the PETRA machine group and the group of the computer center for their excellent support during the experiment and to all the engineers and technicians of the collaborating institutions who have participated in the construction and maintenance of the apparatus. This experiment was supported by the Bundesministerium für Forschung und Technologie, by the Ministry of Education, Science and Culture of Japan, by the UK Science and Engineering Research Council through the Rutherford Appleton Laboratory and by the US Department of Energy. The visiting groups at DESY wish to thank the DESY directorate for the hospitality extended to them.

References

[1] J. Wess and B. Zumino, Nucl. Phys. B70 (1974) 39; Phys. Lett. 49B (1974) 52;
A. Salam and B. Strathdee, Phys. Rev. D11 (1975) 1521;
P. Fayet and S. Ferrara, Phys. Rep. 32C (1977) 249.

[2] S. Dimopoulos and H. Georgi, Nucl. Phys. B193 (1981) 150;
N. Sakai, Z. Phys. C11 (1982) 153.

[3] J. Ellis, SLAC-PUB-3006 (1982);
J. Ellis, L.E. Ibáñez and G.G. Ross, Nucl. Phys. B221 (1983) 29, and references cited therein.

[4] P. Fayet, Phys. Lett. 84B (1979) 416; 86B (1979) 272;
G.R. Farrar and P. Fayet, Phys. Lett. 89B (1980) 191.

[5] L.E. Ibáñez and G.G. Ross, Phys. Lett. 110B (1982) 215;
J. Ellis, L.E. Ibáñez and G.G. Ross, Phys. Lett. 113B (1982) 283;
J. Ellis, J.S. Hagelin and D.V. Nanopoulos, Phys. Lett. 116B (1982) 283.

[6] JADE Collab., D. Cords, Proc. XXth Intern. Conf. on High energy physics (Madison, Wisconsin, 1980), p. 590;
PLUTO Collab., H. Spitzer, Proc. XVth Rencontre de Moriond, ed. J. Tran Thanh Van (Les Arcs, 1980);

CELLO Collab., H.J. Behrend et al., Phys. Lett. 114B (1982) 287;
TASSO Collab., R. Brandelik et al., Phys. Lett. 117B (1982) 365.
[7] L. Gladney et al., Phys. Rev. Lett. 51 (1983) 2253;
E. Fernandez et al., Phys. Rev. Lett. 52 (1984) 22.
[8] M.K. Gaillard, L. Hall and I. Hinchliffe, Phys. Lett. 116B (1982) 279.
[9] N. Cabibbo, G.R. Farrar and L. Maiani, Phys. Lett. 105B (1981) 155.
[10] CELLO Collab., H.J. Behrend et al., Phys. Lett. 123B (1983) 127.
[11] JADE Collab., W. Bartel et al., Phys. Lett. 139B (1984) 327.
[12] TASSO Collab., M. Althoff et al., DESY 1984-72.
[13] H. Takeda, EPS meeting (Brighton, UK, 1983);
S. Yamada, Proc. Intern. Symp. on Lepton and photon interactions at high energies (Cornell, Ithaca, NY, USA, 1983) p. 525.
[14] JADE Collab., W. Bartel et al., Phys. Lett. 152B (1985) 392.
[15] JADE Collab., W. Bartel et al., Phys. Lett. 88B (1979) 171; 92B (1980) 206.
[16] T. Kobayashi and M. Kuroda, Phys. Lett. 134B (1984) 271.
[17] I. Hinchliffe and L. Littenberg, LBL-15022 (1982).
[18] JADE Collab., W. Bartel et al., Phys. Lett. 108B (1982) 140;
JADE Collab., A.H. Ball, Proc. Intern. Europhysics Conf. on High energy physics (Brighton, UK, July 1983).
[19] T. Kobayashi and M. Kuroda, Phys. Lett. 139B (1984) 208;
J.D. Ware and M.E. Machacek, Phys. Lett. 142B (1984) 301.
[20] M. Glück and E. Reya, Phys. Lett. 130B (1983) 423.